Fractional quantum Hall effect in a quantum point contact at filling fraction 5/2

JEFFREY B. MILLER[1], IULIANA P. RADU[2], DOMINIK M. ZUMBÜHL[2,3], ELI M. LEVENSON-FALK[4], MARC A. KASTNER[2], CHARLES M. MARCUS[4]*, LOREN N. PFEIFFER[5] AND KEN W. WEST[5]

[1]Division of Engineering and Applied Science, Harvard University, Cambridge, Massachusetts 02138, USA
[2]Department of Physics, Massachusetts Institute of Technology, Cambridge, Massachusetts 02139, USA
[3]Department of Physics and Astronomy, University of Basel, Klingelbergstrasse 82, CH-4056 Basel, Switzerland
[4]Department of Physics, Harvard University, Cambridge, Massachusetts 02138, USA
[5]Bell Labs, Lucent Technologies, Murray Hill, New Jersey 07974, USA
*e-mail: marcus@harvard.edu

Published online: 1 July 2007; doi:10.1038/nphys658

Recent theories suggest that the quasiparticles that populate certain quantum Hall states should exhibit exotic braiding statistics that could be used to build topological quantum gates. Confined systems that support such states at a filling fraction $\nu = 5/2$ are of particular interest for testing these predictions. Here, we report transport measurements of just such a system, which consists of a quantum point contact (QPC) in a two-dimensional GaAs/AlGaAs electron gas that itself exhibits a well-developed fractional quantum Hall effect at a bulk filling fraction $\nu_{bulk} = 5/2$. We observe plateau-like features at an effective filling fraction of $\nu_{QPC} = 5/2$ for lithographic contact widths of 1.2 μm and 0.8 μm, but not 0.5 μm. Transport near $\nu_{QPC} = 5/2$ in the QPCs is consistent with a picture of chiral Luttinger-liquid edge states with inter-edge tunnelling, suggesting that an incompressible state at $\nu_{QPC} = 5/2$ forms in this confined geometry.

The discovery[1] of a fractional quantum Hall effect (FQHE) at the even-denominator filling fraction $\nu = 5/2$ has sparked a series of experimental[2–6] and theoretical[7–9] studies, leading to a prevailing interpretation of the 5/2 state as comprising paired fermions condensed into a Bardeen–Cooper–Schrieffer-like state[10–13]. Within this picture, excitations of the 5/2 ground state possess non-abelian statistics[14–16] and associated topological properties. The possibility that such a topological state can be accessed in the laboratory has prompted recent theoretical work aimed at experimentally testing the non-abelian character of the 5/2 state[17–21], and building topologically protected quantum gates controlled by manipulating the excitations of the 5/2 state[22–24].

Whereas proposed tests of the statistics of excitations of the 5/2 state make use of confined (∼few micrometre) geometries, previous studies of the 5/2 state have been conducted in macroscopic (100 μm–5 mm) samples. Although experiments using mesoscopic samples with a quantum point contact (QPC) are now routine, the 5/2 state is exceptionally fragile; only the highest quality GaAs/AlGaAs heterostructures exhibit a 5/2 state even in bulk samples. Experimental investigation of the statistics of the 5/2 ground state is crucial, especially because alternative models have been proposed to explain the 5/2 state in confined geometries[25] and in the bulk[12,26].

In this paper, we study the 5/2 state in the vicinity of a QPC. Near a QPC, the electron density is not uniform, so the notion of a QPC filling fraction is not well defined. However, on the basis of transport measurements, it is possible to define an effective filling fraction in the vicinity of the QPC (ν_{QPC}), as discussed below. Below 30 mK, a plateau-like feature with diagonal resistance (also defined below) near, but above, the bulk quantized value of $0.4\,h/e^2$ is evident at $\nu_{QPC} = 5/2$ in QPCs with 1.2 μm and 0.8 μm spacings between the gates. On this plateau, we find a peak in the differential resistance at d.c.-current bias $I_{d.c.} = 0$ and a dip around $I_{d.c.} \sim 1.2$ nA, a characteristic shape that is consistent with QPC-induced quasiparticle tunnelling between fractional edge states[27]. We also observe a zero-bias peak at $\nu_{QPC} = 7/3$, whereas we find a zero-bias dip near $\nu_{QPC} = 8/3$ (not shown), consistent with previous QPC studies for $\nu_{QPC} < 1$ (ref. 28). As the temperature increases from 30 mK to 70 mK, the plateaux in the QPC disappear. Fractional plateaux are not observed in a 0.5 μm QPC, and the $I_{d.c.}$ characteristic is flat for all magnetic fields. Together, these observations suggest that the 5/2 state is destroyed in the 0.5 μm QPC, but can survive and exhibit quasiparticle tunnelling[28–30] in the larger QPCs.

R_{xy}, R_{xx}, R_D and R_L (Fig. 1) are four-wire differential resistances ($R = dV/dI_{a.c.}$), measured at $I_{d.c.} = 0$ unless otherwise noted. In the integer quantum Hall effect (IQHE) regime, these resistances can be readily interpreted in terms of edge channels[31,32] (see the discussions in sections IV. B and IV. C of ref. 32, in which our R_D here corresponds to R_D^+), where N_{bulk} is the number of edge channels in the bulk and $N_{QPC} (\leq N_{bulk})$ is the number traversing the QPC. The bulk Hall resistance, $R_{xy} \sim h/e^2(1/N_{bulk})$, probes the number of edge states in the bulk region. In the absence of tunnelling across the Hall bar, $R_{xy} = h/e^2(1/N_{bulk})$. The bulk longitudinal resistance, R_{xx}, vanishes when R_{xy} shows a plateau. The diagonal resistance across a QPC, $R_D \sim h/e^2(1/N_{QPC})$, is sensitive only to the number of edge channels traversing the QPC, and hence provides a QPC analogue to the bulk R_{xy}. The longitudinal resistance across the QPC, $R_L \sim R_D - R_{xy}$, contains information about both the bulk and the QPC region, and is not directly analogous to the

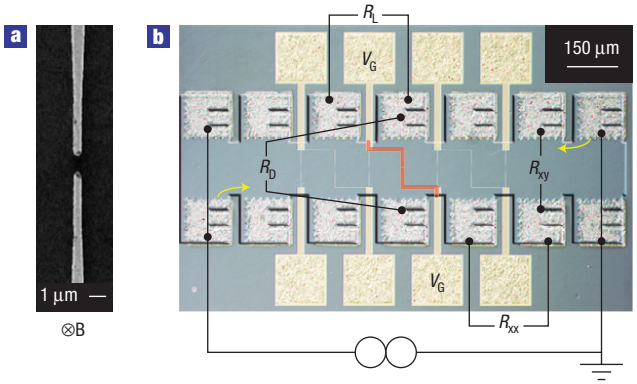

Figure 1 Device and measurement set-up. a, Scanning electron micrograph of the 0.5 μm QPC. **b**, Optical micrograph of the entire device (the outline of the wet-etched Hall bar has been enhanced for clarity). The measurement circuit for the red-highlighted QPC is drawn schematically, with the direction of the edge-current flow indicated by the yellow arrows.

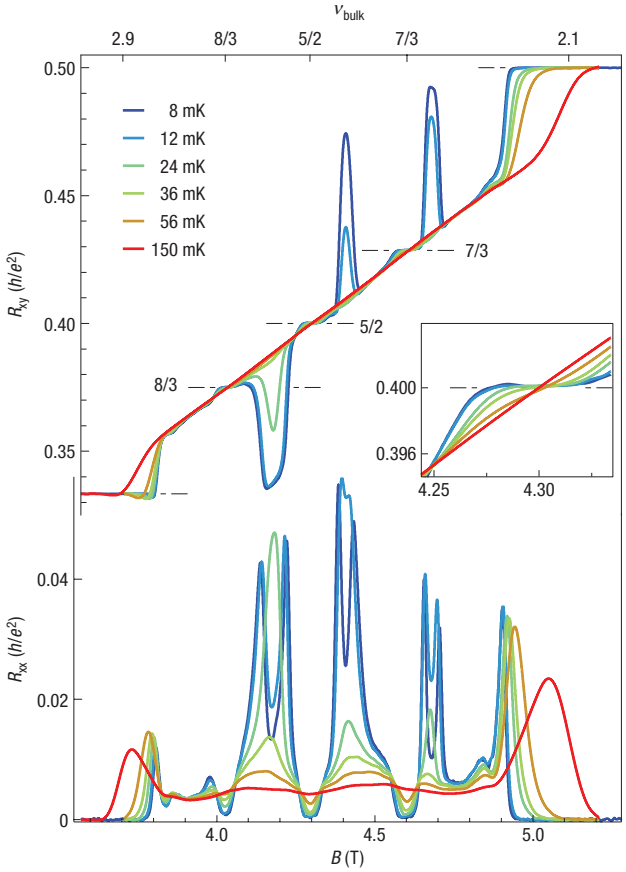

Figure 2 Bulk transport measurements, including *T* dependence. (*T* refers to the temperature of the refrigerator.) The inset is an enlargement of the R_{xy} data near $\nu_{bulk} = 5/2$.

bulk R_{xx}. On bulk IQHE plateaux, the filling fraction is equivalent to the number of edge states, $\nu_{bulk} = N_{bulk}$. By analogy, in the QPC, where the filling fraction is not well defined owing to non-uniform density, we define an effective filling fraction in the QPC: $\nu_{QPC} \sim h/e^2(1/R_D)$.

The edge-state interpretation for R_{xy}, R_{xx}, R_D and R_L has been extended to the FQHE[32–39]. Within this generalized picture, a quantized plateau in $R_{xy} \sim h/e^2(1/\nu_{bulk})$ corresponds to the quantum Hall state at filling fraction ν_{bulk}, and a plateau in $R_D \sim h/e^2(1/\nu_{QPC})$ indicates that an incompressible quantum Hall state has formed in the vicinity of the QPC with effective filling fraction ν_{QPC}. We associate deviations from precisely quantized values with tunnelling, which we study below as a function of temperature and bias.

To simplify the study of quantum states in the vicinity of the QPC, the perpendicular magnetic field (B) and gate voltage of the QPC (V_g) are tuned such that ν_{bulk} is fixed at an IQHE plateau whenever ν_{QPC} is at a value of interest. With $R_{xx} \sim 0$ and R_{xy} quantized to an IQHE plateau, features in R_D and R_L measurements can be attributed to the QPC region and not the bulk.

Previously, QPCs have been used to selectively transmit integer[40,41] and fractional edge channels[36,42], and to study inter-edge tunnelling between fractional edge channels, including in the regime where the bulk is intentionally set to an IQHE plateau[28,43]. Comparisons with these results are discussed below. QPCs have also been used in studies of noise[44,45] and (along with etched trenches) interference of quasiparticles[46] in the FQHE regime. In all of these studies, $\nu < 2$, where the FQHE gaps are typically much larger than those with $\nu > 2$.

The sample is a GaAs/AlGaAs heterostructure grown in the [001] direction with an electron gas layer 200 nm below the surface, with Si δ-doping layers 100 and 300 nm below the surface. A 150-μm-wide Hall bar is patterned using photolithography and a H_2O:H_2SO_4:H_2O_2 (240:8:1) wet-etch, followed by thermally evaporated Cr/Au (5 nm/15 nm) top gates patterned using electron-beam lithography (see Fig. 1). The gates form QPCs with lithographic separation between gates of 0.5, 0.8 and 1.2 μm. Depleting the electron gas beneath only one side of a QPC has no effect on transport measurements. Gate voltages are restricted to the range −1.9 V (depletion) to −3 V and are allowed to stabilize for several hours at each set-point before measuring; beyond −3 V the conductance is typically hysteretic as a function of gate voltage. Measurements are carried out in a dilution refrigerator with a base temperature of 8 mK using standard four-wire lock-in techniques, with an a.c. current-bias excitation ($I_{a.c.}$) ranging from 0.2 to 0.86 nA, and a d.c. current bias ranging from 0 to 20 nA. The differential resistances ($dV/dI_{a.c.}$) are measured in four places, as shown in Fig. 1. All quoted temperatures are measured using a RuO_2 resistor mounted on the mixing chamber. The bulk mobility of the device measured at the base temperature is 2,000 $m^2\,V^{-1}\,s^{-1}$ and the electron density is $2.6 \times 10^{15}\ m^{-2}$.

Bulk R_{xx} and R_{xy} measurements for the filling fraction range $\nu_{bulk} = 3$–2, measured in the vicinity of the 1.2 μm QPC before the gates are energized, are shown in Fig. 2. R_{xx} and R_{xy} are also measured in a region of the Hall bar without gates, and found to be virtually indistinguishable, showing that the surface gates do not significantly affect the two-dimensional electron gas. R_{xx} and R_{xy} in an ungated region show no changes caused by energizing gates.

As temperature is increased, R_{xy} near $\nu_{bulk} = 5/2$ evolves from a well-defined plateau at $R_{xy} = 0.4 \pm 0.0002\ h/e^2$ to a line consistent with the classical Hall effect for a material with this density. There is a stationary point in the middle of the plateau where R_{xy} is very close to $0.4\ h/e^2$, consistent with scaling seen in other quantum Hall transitions[47]. Activation energies, Δ, for the three fractional states $\nu_{bulk} = 5/2$, 7/3 and 8/3 are extracted from the linear portion of the data in a plot of $\ln(R_{xx})$ versus $1/T$ (using the minimum R_{xx} for each FQHE state, and $R_{xx} \propto e^{-\Delta/2T}$), giving

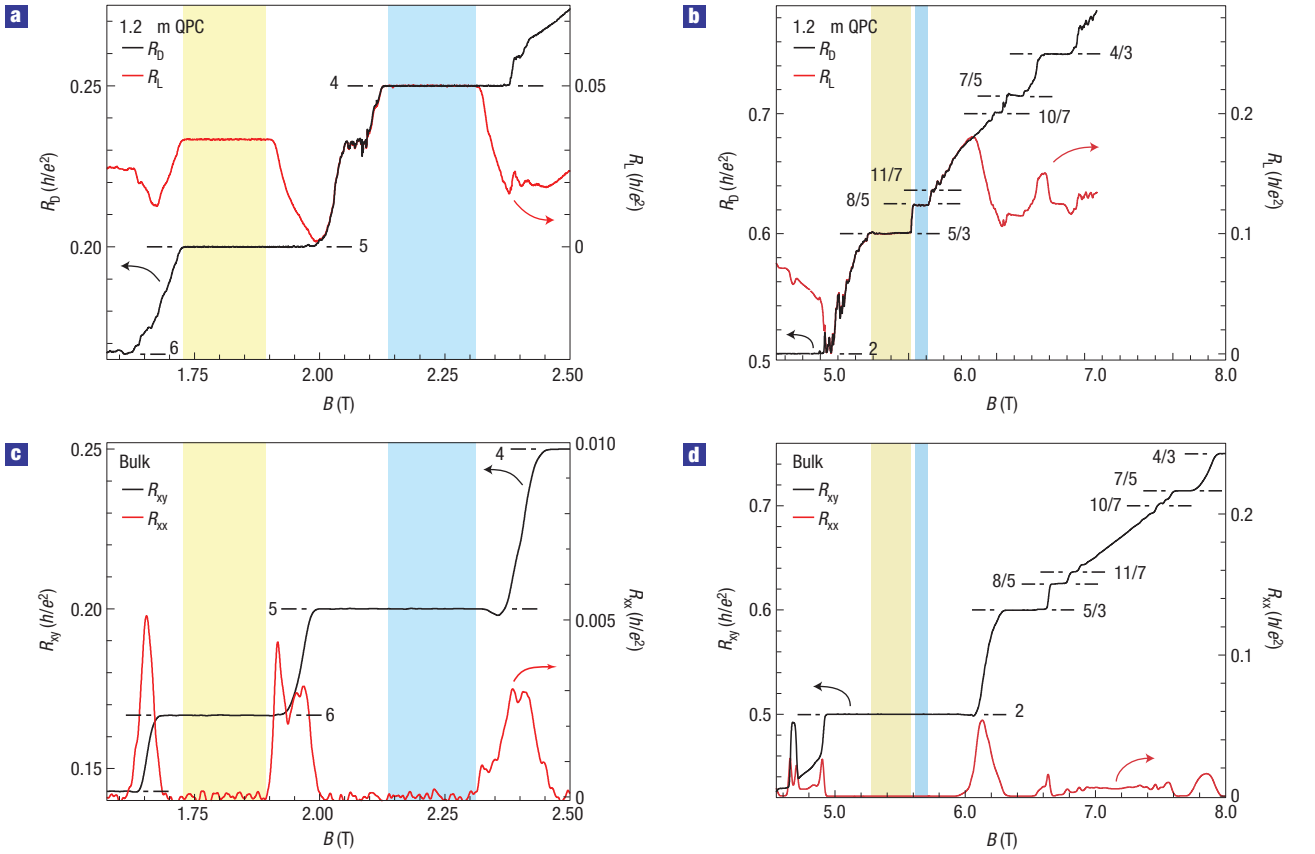

Figure 3 Action of the QPC, compared with concurrent bulk measurements. a–d, Typical magnetoresistance curves measured concurrently in the QPC and the bulk at low magnetic field (**a**,**c**) and high magnetic field (**b**,**d**). Quantized resistance values are indicated in units of h/e^2. The coloured stripes indicate field ranges where one quantum Hall state exists in the QPC while a different quantum Hall state exists in the bulk. All data is for $T \sim 8$ mK.

$\Delta_{8/3} \sim 60$ mK, $\Delta_{5/2} \sim 130$ mK and $\Delta_{7/3} \sim 110$ mK, consistent with previous measured values[1,48,49].

We now focus on measurements with one QPC formed, as shown in Fig. 1. Low-field R_D and R_L data from the 1.2 μm QPC along with concurrently measured R_{xy} and R_{xx} show regions where one IQHE state forms in the bulk with a lower IQHE state in the QPC (see Fig. 3a,c). Figure 3a also shows the appearance of a plateau-like feature in the QPC between $\nu_{QPC} = 5$ and $\nu_{QPC} = 4$ in both the 1.2 μm and 0.8 μm QPCs, which remains unexplained. At higher magnetic fields (Fig. 3b,d), R_D and R_L show FQHE plateaux, whereas the bulk is quantized at the IQHE value $\nu_{bulk} = 2$.

We now concentrate on the range $\nu_{QPC} = 3$ to $\nu_{QPC} = 2$ with $\nu_{bulk} = 3$ (Fig. 4). A plateau-like structure near $\nu_{QPC} = 5/2$ is evident in the 1.2 μm and 0.8 μm QPCs, but is not seen in the 0.5 μm QPC. Near $\nu_{QPC} = 7/3$, we also see plateau-like behaviour in the 1.2 μm QPC, and less well-developed plateaux in the 0.8 μm QPC (although ν_{bulk} is not on a plateau when $\nu_{QPC} \sim 7/3$), but again these features are suppressed in the 0.5 μm QPC. We do not observe any plateaux near $\nu_{QPC} = 8/3$ in any of the QPCs. The re-entrant integer quantum Hall effect features, which are clearly visible in the bulk, do not survive at all in the QPCs.

We interpret the plateau-like features in the two larger QPCs as indicating that the incompressible states at $\nu_{QPC} = 5/2$ and $\nu_{QPC} = 7/3$ are not destroyed by the confinement. The linear, plateau-less behaviour in the 0.5 μm QPC is reminiscent of a classical Hall line, suggesting that no incompressible states survive in this QPC.

The temperature dependence for a representative V_g setting of the 1.2 μm QPC is shown in Fig. 5. Below 30 mK, a distinct plateau-like feature is evident. This plateau disappears between 30 and 70 mK, consistent with the disappearance of the plateaux in the bulk. However, unlike the bulk, where the 5/2 plateau disappears symmetrically around a stationary point at $R_{xy} = 0.4\,h/e^2$ as temperature increases, in the QPC there is a further resistance: R_D exceeds the quantized value of $0.4\,h/e^2$ by $26\,\Omega \pm 5\,\Omega$. We also note that the extra resistance on the plateau decreases as the temperature increases, behaviour consistently observed in both the 0.8 μm and 1.2 μm QPCs. We interpret this as indicating that the temperature dependence comes not only from the thermal excitation of quasiparticles, but also from the temperature dependence of their backscattering.

The dependence of the differential resistance on the d.c. source–drain bias, $I_{d.c.}$, (Fig. 6) provides further insight into this excess resistance. At the base temperature, the resistances R_D versus $I_{d.c.}$ near $\nu_{QPC} = 5/2$ and $\nu_{QPC} = 7/3$ in the 1.2 μm (Fig. 6) and 0.8 μm (not shown) QPCs show a pronounced peak at $I_{d.c.} = 0$, a dip at intermediate values and saturation to a constant value at high currents. In these QPCs, the $I_{d.c.}$ behaviour near $\nu_{QPC} = 8/3$ (not shown) is inverted, with a pronounced dip at $I_{d.c.} = 0$, a peak at intermediate values and high-current saturation. In the 0.5 μm QPC, the $I_{d.c.}$ traces are flat for all filling fractions between $\nu_{QPC} = 3$ and $\nu_{QPC} = 2$. All of the traces in Fig. 6 are measured with an a.c. lock-in excitation $I_{a.c.} = 0.2$ nA (whereas the data in all other figures are measured with $I_{a.c.} = 0.86$ nA).

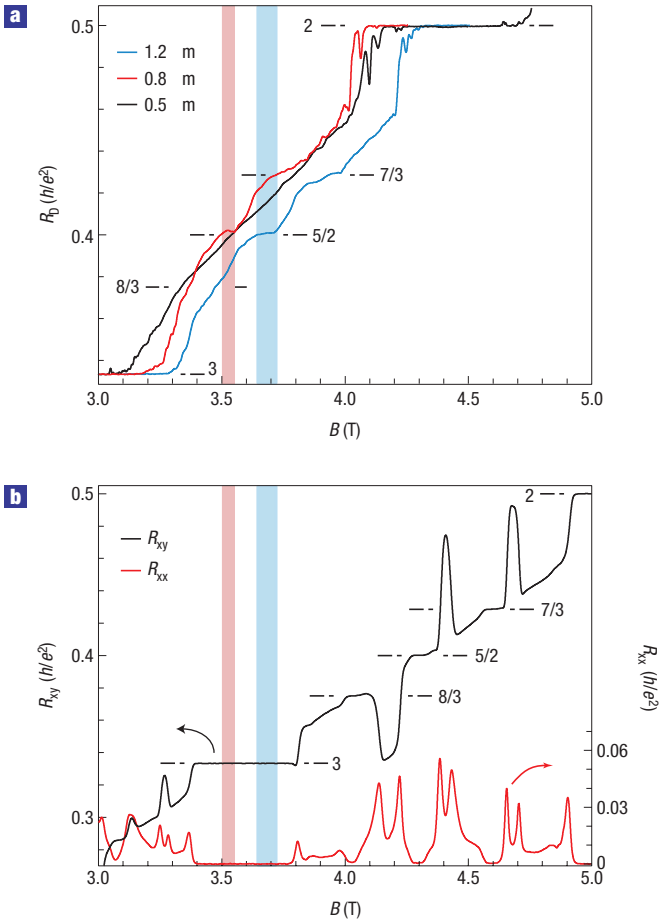

Figure 4 Observation of structure near quantized values in various QPCs. **a**,**b**, Typical magnetoresistance from $\nu = 3$ to $\nu = 2$, measured concurrently in various QPCs (**a**) and the bulk (**b**). In **a**, the R_D curves are from three different QPCs, of lithographic size 0.5 μm (black), 0.8 μm (red) and 1.2 μm (blue). The coloured stripes highlight regions in the field where the resistance in the 1.2 μm and 0.8 μm QPCs forms a plateau-like feature near $\nu_{QPC} = 5/2$ with $\nu_{bulk} = 3$. The applied gate voltages, V_g, are −2.2, −2.0 and −1.9 V for the 1.2, 0.8 and 0.5 μm QPCs and the a.c. lock-in excitation is 0.86 nA. All data is for $T \sim 8$ mK.

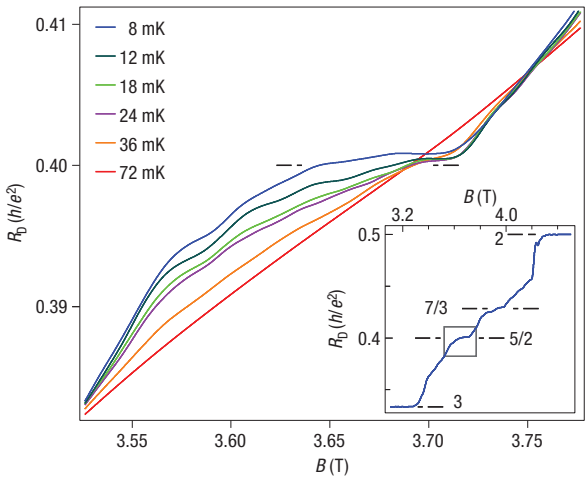

Figure 5 Temperature dependence of the 5/2 state in the 1.2 μm QPC. The inset shows an expanded range of the 8 mK trace with the grey square indicating the range of the data in the main panel. All traces are measured with $V_g = -2.7$ V and an a.c. lock-in excitation of 0.86 nA. $\nu_{bulk} = 3$ for the entire B range of the main panel, but not the full range of the inset.

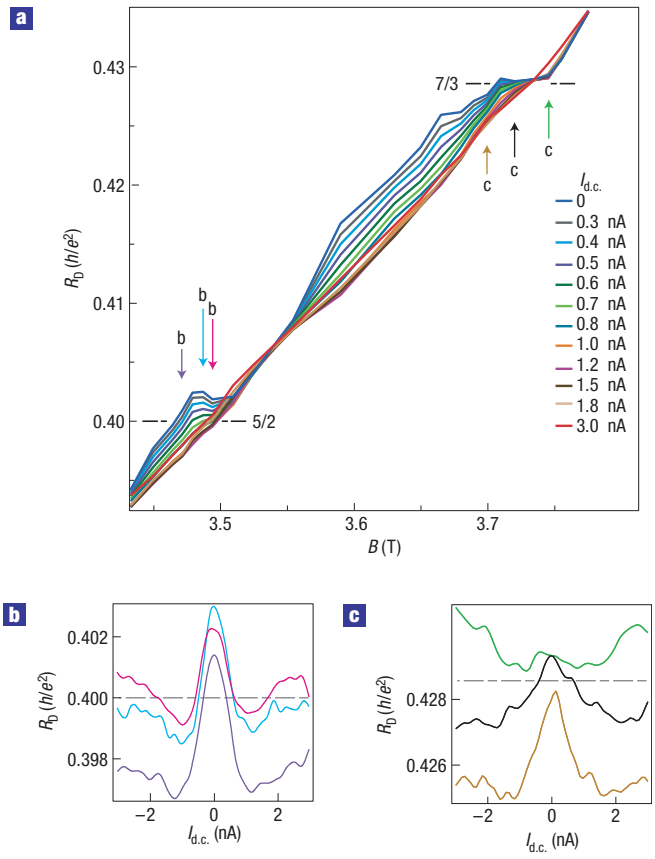

Figure 6 Dependence on d.c. current bias of the 5/2 and 7/3 states in the 1.2 μm QPC. **a**, The R_D data as a function of magnetic field; each trace represents a different $I_{d.c.}$ from 0 nA to 3 nA. **b**,**c**, R_D as a function of $I_{d.c.}$ for selected magnetic fields (indicated by the colour-coded arrows). The dashed grey lines indicate resistance values of $(2/5)h/e^2$ (**b**) and $(3/7)h/e^2$ (**c**). All traces are measured at $T \sim 8$ mK with $V_g = -2.4$ V and an a.c. lock-in excitation of 0.2 nA. $\nu_{bulk} = 3$ for all fields shown in this figure.

Figure 6 provides a key point of comparison to previous experimental and theoretical work on the FQHE. In a recent experiment[28], a QPC is used to measure tunnelling differential resistance characteristics ($I_{d.c.}$ curves) for $\nu_{QPC} < 1$ while ν_{bulk} is fixed on an IQHE plateau. Our $I_{d.c.}$ data for $2 < \nu_{QPC} < 3$ and $\nu_{bulk} = 3$, with a distinct peak at zero bias and dips at intermediate biases, resembles the $I_{d.c.}$ curves in that work. In ref. 28, it is convincingly argued that the $I_{d.c.}$ curves are a signature of quasiparticle tunnelling between the FQHE edge states, on the basis of a quantitative comparison to applicable theory. That theory states that the characteristic for tunnelling between FQHE edge states[27,37,50] is expected to have a peak at zero bias and a minimum at intermediate biases, whereas tunnelling between IQHE edge channels is expected to yield a flat (ohmic) curve. The data we present for $\nu_{QPC} = 5/2$, both the temperature dependence and the $I_{d.c.}$ curves, are consistent with the formation of an FQHE state with tunnelling-related backscattering.

We interpret that a mechanism for the deviation of R_D from $0.4\,h/e^2$ near 5/2 and 7/3, as well as the peak-and-dip behaviour of the $I_{d.c.}$ data, could be tunnelling between edge channels on

opposite sides of the Hall bar in the vicinity of the QPC. We do not believe that the data can be explained by transport via thermally excited particles through the (small) bulk region of the QPC, as this process would be expected to have the opposite temperature dependence.

Received 7 March 2007; accepted 25 May 2007; published 1 July 2007.

References

1. Willett, R. *et al.* Observation of an even-denominator quantum number in the fractional quantum Hall effect. *Phys. Rev. Lett.* **59**, 1776–1779 (1987).
2. Eisenstein, J. P. *et al.* Collapse of the even-denominator fractional quantum Hall effect in tilted fields. *Phys. Rev. Lett.* **61**, 997–1000 (1988).
3. Eisenstein, J. P., Willett, R., Störmer, H. L., Pfeiffer, L. N. & West, K. W. Activation energies for the even-denominator fractional quantum Hall effect. *Surf. Sci.* **229**, 31–33 (1990).
4. Pan, W. *et al.* Exact quantization of the even-denominator fractional quantum Hall state at $\nu = 5/2$ Landau level filling factor. *Phys. Rev. Lett.* **83**, 3530–3533 (1999).
5. Pan, W. *et al.* Strongly anisotropic electronic transport at Landau level filling factor $\nu = 9/2$ and $\nu = 5/2$ under a tilted magnetic field. *Phys. Rev. Lett.* **83**, 820–823 (1999).
6. Lilly, M. P., Cooper, K. B., Eisenstein, J. P., Pfeiffer, L. N. & West, K. W. Anisotropic states of two-dimensional electron systems in high Landau levels: Effect of an in-plane magnetic field. *Phys. Rev. Lett.* **83**, 824–827 (1999).
7. Haldane, F. D. M. & Rezayi, E. H. Spin-singlet wave function for the half-integral quantum Hall effect. *Phys. Rev. Lett.* **60**, 956–959 (1988).
8. Morf, R. H. Transition from quantum Hall to compressible states in the second Landau level: New light on the $\nu = 5/2$ enigma. *Phys. Rev. Lett.* **80**, 1505–1508 (1998).
9. Rezayi, E. H. & Haldane, F. D. M. Incompressible paired Hall state, stripe order, and the composite fermion liquid phase in half-filled Landau levels. *Phys. Rev. Lett.* **84**, 4685–4688 (2000).
10. Moore, G. & Read, N. Nonabelions in the fractional quantum Hall effect. *Nucl. Phys. B* **360**, 362–396 (1991).
11. Greiter, M., Wen, X.-G. & Wilczek, F. Paired Hall state at half filling. *Phys. Rev. Lett.* **66**, 3205–3208 (1991).
12. Read, N. & Green, D. Paired states of fermions in two dimensions with breaking of parity and time-reversal symmetries and the fractional quantum Hall effect. *Phys. Rev. B* **61**, 10267–10297 (2000).
13. Scarola, V. W., Park, K. & Jain, J. K. Cooper instability of composite fermions. *Nature* **406**, 863–865 (2000).
14. Nayak, C. & Wilczek, F. 2*n*-quasihole states realize 2^{n-1}-dimensional spinor braiding statistics in paired quantum Hall states. *Nucl. Phys. B* **479**, 529–553 (1996).
15. Tserkovnyak, Y. & Simon, S. H. Monte Carlo evaluation of non-abelian statistics. *Phys. Rev. Lett.* **90**, 016802 (2003).
16. Stern, A., von Oppen, F. & Mariani, E. Geometric phases and quantum entanglement as building blocks for non-abelian quasiparticle statistics. *Phys. Rev. B* **70**, 205338 (2004).
17. Stern, A. & Halperin, B. I. Proposed experiments to probe the non-abelian $\nu = 5/2$ quantum Hall state. *Phys. Rev. Lett.* **96**, 016802 (2006).
18. Bonderson, P., Kitaev, A. & Shtengel, K. Detecting non-abelian statistics in the $\nu = 5/2$ fractional quantum Hall state. *Phys. Rev. Lett.* **96**, 016803 (2006).
19. Hou, C.-Y. & Chamon, C. 'Wormhole' geometry for entrapping topologically protected qubits in non-abelian quantum Hall states and probing them with voltage and noise measurements. *Phys. Rev. Lett.* **97**, 146802 (2006).
20. Chung, S. B. & Stone, M. Proposal for reading out anyon qubits in non-abelian $\nu = 12/5$ quantum Hall state. *Phys. Rev. B* **73**, 245311 (2006).
21. Feldman, D. E. & Kitaev, A. Detecting non-abelian statistics with an electronic Mach-Zender interferometer. *Phys. Rev. Lett.* **97**, 186803 (2006).
22. Kitaev, A. Anyons in an exactly solved model and beyond. *Ann. Phys. (N.Y.)* **321**, 2–111 (2006).
23. Bonesteel, N. E., Hormozi, L., Zikos, G. & Simon, S. H. Braid topologies for quantum computation. *Phys. Rev. Lett.* **95**, 140503 (2005).
24. Das Sarma, S., Freedman, M. & Nayak, C. Topologically protected qubits from a possible non-abelian fractional quantum Hall state. *Phys. Rev. Lett.* **94**, 166802 (2005).
25. Harju, A., Saarikoski, H. & Räsänen, E. Half-integer filling-factor states in quantum dots. *Phys. Rev. Lett.* **96**, 126805 (2006).
26. Töke, C. & Jain, J. K. Understanding the 5/2 fractional quantum Hall effect without the pfaffian wave function. *Phys. Rev. Lett.* **96**, 246805 (2006).
27. Fendley, P., Ludwig, A. W. W. & Saleur, H. Exact nonequilibrium transport through point contacts in quantum wires and fractional quantum Hall devices. *Phys. Rev. B* **52**, 8934–8950 (1995).
28. Roddaro, S., Pellegrini, V., Beltram, F., Pfeiffer, L. N. & West, K. W. Particle-hole symmetric Luttinger liquids in a quantum Hall circuit. *Phys. Rev. Lett.* **95**, 156804 (2005).
29. Fendley, P., Fisher, M. P. A. & Nayak, C. Dynamical disentanglement across a point contact in a non-abelian quantum Hall state. *Phys. Rev. Lett.* **97**, 036801 (2006).
30. D'Agosta, R., Vignale, G. & Raimondi, R. Temperature dependence of the tunneling amplitude between quantum Hall edges. *Phys. Rev. Lett.* **94**, 086801 (2005).
31. Büttiker, M. Four-terminal phase-coherent conductance. *Phys. Rev. Lett.* **57**, 1761–1764 (1986).
32. Beenakker, C. W. J. & van Houten, H. Quantum transport in semiconductor nanostructures. *Solid State Phys.* **44**, 1–128 (1991).
33. Beenakker, C. W. J. Edge channels for the fractional quantum Hall effect. *Phys. Rev. Lett.* **64**, 216–219 (1990).
34. MacDonald, A. H. Edge states in the fractional-quantum-Hall-effect regime. *Phys. Rev. Lett.* **64**, 220–223 (1990).
35. Chang, A. M. & Cunningham, J. E. Transmission and reflection probabilities between quantum Hall effects and between $\nu = 1$ and $\nu = 2/3$ quantum Hall effects and between $\nu = 2/3$ and $\nu = 1/3$ effects. *Solid State Commun.* **72**, 651–655 (1989).
36. Kouwenhoven, L. P. *et al.* Selective population and detection of edge channels in the fractional quantum Hall regime. *Phys. Rev. Lett.* **64**, 685–688 (1990).
37. Wen, X. G. Electrodynamical properties of gapless edge excitations in the fractional quantum Hall states. *Phys. Rev. Lett.* **64**, 2206–2209 (1990).
38. Wang, J. K. & Goldman, V. J. Edge states in the fractional quantum Hall effect. *Phys. Rev. Lett.* **67**, 749–752 (1991).
39. Würtz, A. *et al.* Separately contacted edge states in the fractional quantum Hall regime. *Physica E* **22**, 177–180 (2004).
40. van Wees, B. J. *et al.* Quantized conductance of magnetoelectric subbands in ballistic point contacts. *Phys. Rev. B* **38**, 3625–3627 (1988).
41. Alphenaar, B. W., McEuen, P. L., Wheeler, R. G. & Sacks, R. N. Selective equilibration among the current-carrying states in the quantum Hall regime. *Phys. Rev. Lett.* **64**, 677–680 (1990).
42. Alphenaar, B. W., Williamson, J. G., van Houten, H., Beenakker, C. W. J. & Foxon, C. T. Observation of excess conductance of a constricted electron gas in the fractional quantum Hall regime. *Phys. Rev. B* **45**, 3890–3893 (1992).
43. Lal, S. On transport in quantum Hall systems with constrictions. Preprint at <http://www.arxiv.org/abs/condmat/0611218> (2006).
44. Saminadayar, L., Glattli, D. C., Jin, Y. & Etienne, B. Observation of the $e/3$ fractionally charged Laughlin quasiparticle. *Phys. Rev. Lett.* **79**, 2526–2529 (1997).
45. de Picciotto, R. *et al.* Direct observation of a fractional charge. *Nature* **389**, 162–164 (1997).
46. Camino, F. E., Zhou, W. & Goldman, V. J. Aharonov–Bohm superperiod in a laughlin quasiparticle interferometer. *Phys. Rev. Lett.* **95**, 246802 (2005).
47. Das Sarma, S. in *Perspectives in Quantum Hall Effects* (eds Das Sarma, S. & Pinczuk, A.) (Wiley, New York, 1997).
48. Eisenstein, J. P., Cooper, K. B., Pfeiffer, L. N. & West, K. W. Insulating and fractional quantum Hall states in the first excited Landau level. *Phys. Rev. Lett.* **88**, 076801 (2002).
49. Xia, J. S. *et al.* Electron correlation in the second Landau level: A competition between many nearly degenerate quantum phases. *Phys. Rev. Lett.* **93**, 176809 (2004).
50. Moon, K., Yi, H., Kane, C. L., Girvin, S. M. & Fisher, M. P. A. Resonant tunneling between quantum Hall edge states. *Phys. Rev. Lett.* **71**, 4381–4384 (1993).

Acknowledgements

We gratefully acknowledge helpful discussions with M. Fisher, B. Halperin, A. Johnson, E.-A. Kim, B. Rosenow, A. Stern, X.-G. Wen and A. Yacoby. This research was supported in part by the Microsoft Corporation Project Q, HCRP at Harvard University, ARO (W911NF-05-1-0062), the NSEC program of the NSF (PHY-0117795) and NSF (DMR-0353209) at MIT.
Correspondence and requests for materials should be addressed to C.M.M.

Competing financial interests

The authors declare no competing financial interests.